Available online at www.sciencedirect.com

ScienceDirect

Procedia Structural Integrity 13 (2018) 1751–1755

Structural Integrity Procedia

www.elsevier.com/locate/procedia

ECF22 - Loading and Environmental effects on Structural Integrity

3D Stress Fields Versus Void Distributions Ahead Of a Notch Tip For Semi-crystalline Polymers

L. Laiarinandrasana[a,*], N. Selles[a], Y. Cheng[b], L. Helfen[b,c], T.F. Morgeneyer[a]

[a] *PSL-Research University, MINES ParisTech, MAT-Centre des Matériaux, CNRS UMR7633, BP 87, F-91003 Evry Cedex, France*

[b] *European Synchrotron Radiation Facility (ESRF), BP 220, F-38043 Grenoble Cedex, France*

[c] *Institute for Photon Science and Synchrotron Radiation (IPS), Karlsruhe Institute of Technology (KIT), D-76344 Eggenstein-Leopoldshafen, Germany*

Abstract

The creep durability of engineering structures relies on the theory of Fracture Mechanics for Creeping Solids (FMCS). The studied material is a semi-crystalline polymer. The lifespan of plastic pipes being generally specified in terms of years of service, its prediction requires reliable constitutive models accounting for time dependent deformation under multiaxial stress states and failure criteria based on the mechanisms of damage and failure. Here, an experimental approach was developed so as to analyze the mechanisms of deformation and cavitation at the microstructural scale by using 3D imaging (tomography/laminography). Three stress triaxiality ratios were addressed using various notched specimen geometries. The void characteristic dimensions (volume fraction, height and diameter) were then measured by defining a volume of interest. The spatial distributions of these characteristics at a prescribed creep time were observed to be dependent on the stress triaxiality ratio. A finite element constitutive model using the porosity as an internal variable, was selected. Comparison of the multiscale experimental database with those simulated at the macroscopic scale as well as at the microstructure level was satisfactory. In the light of the finite element results, the principal stress singularities were in good agreement with the void characteristic lengths.

Peer-review under responsibility of the ECF22 organizers.

Keywords: Type your keywords here, separated by semicolons ;

1. Introduction

Engineering structures made of semi-crystalline polymers are subjected to complex thermo-mechanical loadings. Lifetime prediction in terms of years of service for these industrial structures requires reliable constitutive models of time dependent deformation and multiaxial stress states. Here, a multiscale experimental approach was developed on notched and pre-cracked specimens. The results combined macroscopic data consisting of the creep displacements and data sets at the microstructural scale by using 3D imaging (tomography/laminography). A better understanding of the

* Corresponding author. Tel.: +33-1-60-76-30-64; fax: +33-1-60-76-31-50.
E-mail address: lucien.laiarinandrasana@mines-paristech.fr

2452-3216
Peer-review under responsibility of the ECF22 organizers.
10.1016/j.prostr.2018.12.367

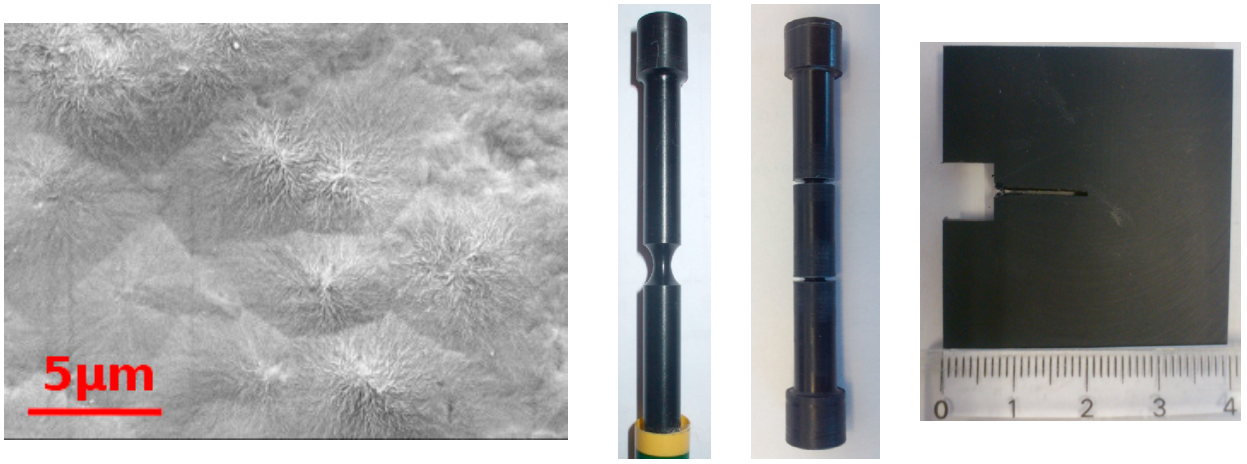

Fig. 1. Material and specimens: a) Spherulitic microstructure; b) Notched round bar with 4 mm notch root radius; c) Notched round bar with 0.45 mm notch root radius; d) CT specimen (thickness=2 mm).

mechanisms of deformation and cavitation was obtained: the void volume fraction was measured by using a prescribed volume of interest. Moreover, the average void heights and diameters within this volume of interest were determined. The spatial distributions of these characteristics were plotted. Instead of using the digital volume correlation technique to compare the strain fields, the approach here consisted of using Finite Element (FE) analysis to correlate the void characteristic lengths to the principal stresses.

2. Experiments

The material studied was a semi-crystalline Polyamide 6 (PA6) with a spherulitic microstructure (fig. 1a) as reported in Laiarinandrasana et al. (2012). Three notched and cracked specimens, described in fig. 1b,c,d, were chosen. They allowed the stress multiaxiality and the profile of the stress gradient in the microstructure to be controlled (Laiarinandrasana et al. (2016)). These specimens were subjected to creep crack growth tests. The failure occurred during the apparent tertiary creep stage. The applied net stress and creep displacement were recorded throughout the tests. Some of the creep tests were stopped at the onset of the tertiary stage. The deformed specimens (after unloading) were inspected using tomography-laminography techniques (Laiarinandrasana et al. (2012), Laiarinandrasana et al. (2016)) to better understand the evolution of spherulitic microstructures during the creep deformation. The mechanisms viewed at the microscopic scale, within a prescribed volume of interest, were then synchronized with the macroscopic strain level. These multiscale experimental data were used to analyze the time dependent deformations involved during creep. A constitutive model accounting for these deformations and implemented in an in-house FE code (Besson and Foerch (1997)) was then used to simulate the creep tests. To this end, the two notched round bars together with the CT specimen were meshed. Attention was paid to make the mesh size in the vicinity of the notch/crack front coincide with the “experimental” volume of interest.

3. Results

3.1. Opening displacement rates

As mentioned above, the opening displacements (δ_c) were recorded during each creep test. The symbols in fig. 2 show some examples of the evolution of (δ_c) as well as that of the opening displacement rate ($d\delta_c/dt$) for the three

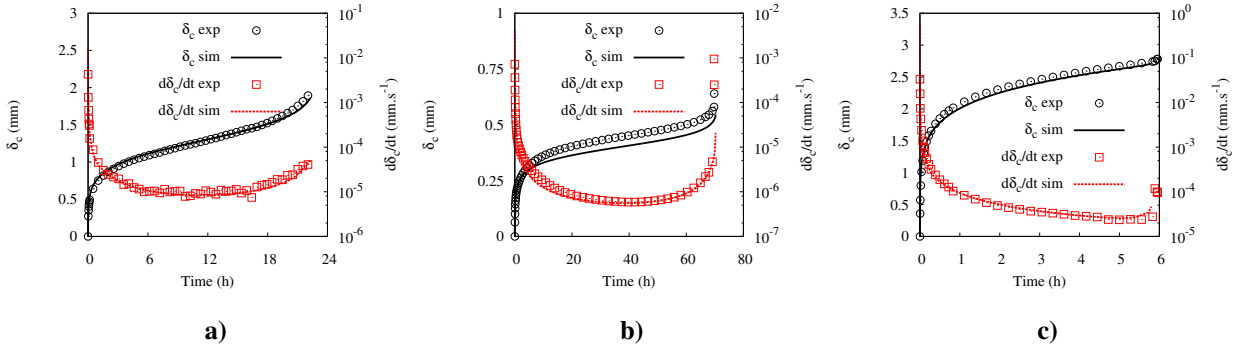

Fig. 2. Notch/Crack opening displacement (rates) for: a) NT4 round bar; b) NT045 round bar; c) CT specimen.

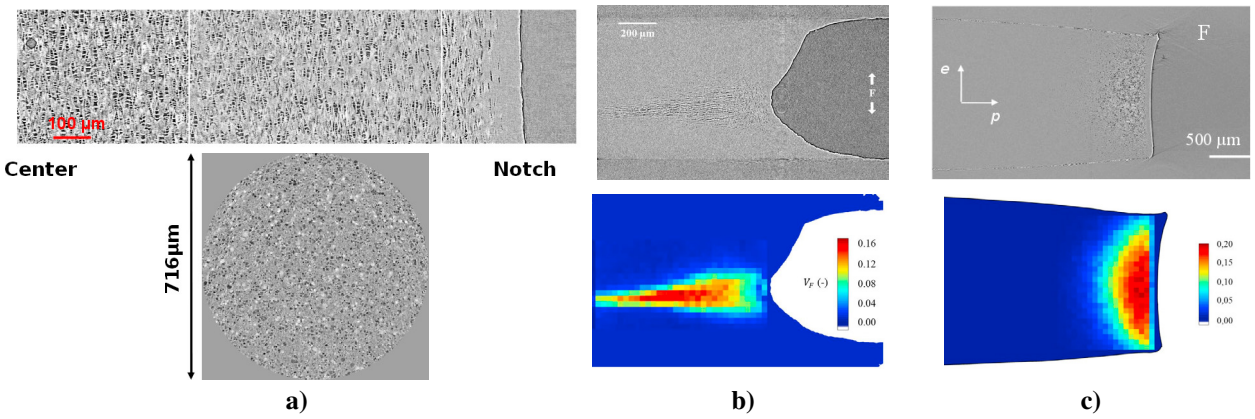

Fig. 3. Void morphology and distribution for: a) NT4 round bar (side and top views); b) NT045 round bar (side view: examinations/measured V_f); c) CT specimen (top view of the fracture surface: examinations/measured V_f).

geometries during the creep tests. Each test in fig. 2 was stopped and unloaded at the last point of the diagram. These data was useful to calibrate the material coefficients in the FE modelling.

3.2. Voiding due to creep

Creep deformed round bars and CT sample were inspected by tomography and laminography respectively. The main results of these examinations were detailed in Selles et al. (2016). The tomography/laminography data sets in fig. 3 summarize the morphology and the distribution of voids (black pixels). For NT4 (fig. 3a), it was observed that voids became more numerous and larger from the surface to the centre. Depending on their location within the net section, voids were cylindrical with variable height (h_v) and diameter (ϕ). For NT045, Selles et al. (2017) described the data treatment allowing the distribution of V_f to be displayed as a contour map shown in fig. 3b (bottom). In this geometry, it was clearly indicated that the maximum void volume fraction V_f was located in between the centre and the notch root radius, in opposition to what was observed on NT4. Moreover, for this high triaxiality geometry most of voids were penny shaped. For the CT specimen inspected by laminography (fig. 3c), the crack front was not straight but slightly curved (deviation of about 100 µm). Additionally, a significant thickness reduction was observed near the crack front. The contour map indicates that the maximum V_f was located at the mid-thickness and at a small distance ahead of the crack front.

Further to the V_f distributions, the individual void height (h_v) and diameter (ϕ) were plotted with respect to its position in a cylindrical coordinate: (r, θ, z) where z is the load direction. As it is straightforward for the round bars, these characteristic lengths were plotted according to the normalized radius of the net section r/R. For CT specimen,

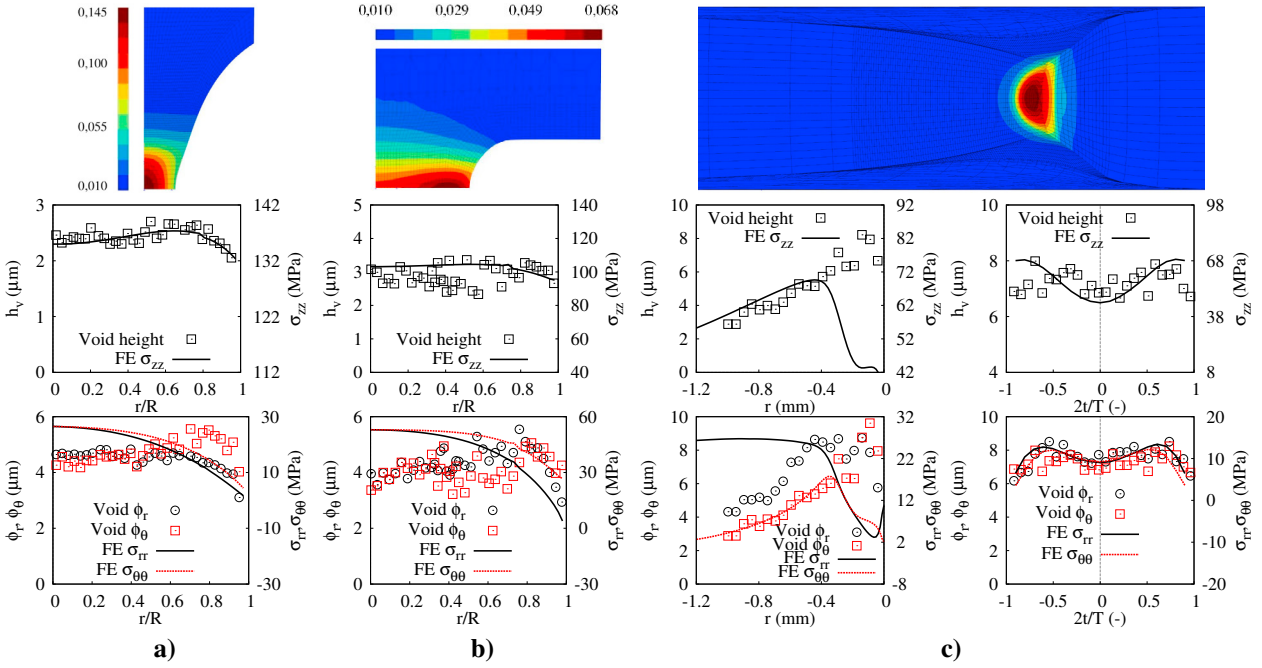

Fig. 4. Void height (h_v) and diameter (ϕ) *vs.* principal stress through the 3 directions of the coordinates (z being the load direction). From top to bottom, porosity contour maps, void height *vs.* maximum principal stress σ_{zz}, void diameters *vs.* transverse stresses: a) NT4 round bar; b) NT045 round bar; c) CT specimen.

r and θ corresponded to the crack propagation and the thickness directions respectively. h_v and ϕ were the plotted through r and through the normalized thickness coordinate (2t/T).

The main results are illustrated in the bottom rows of diagrams in figs. 4a,b,c. The symbols (open squares and circles) represent the void characteristic lengths corresponding to the first Y-axis. As mentioned earlier voids were cylindrical showing here a 3D shape with a "unique" height but with an elliptical basis, thus two diameters: ϕ_r, ϕ_θ. For NT4 and NT045 notched round bars (figs. 4a,b), it was observed that the circumferential diameter ϕ_θ was the major axis, that is, greater than ϕ_r. The diagram relative to the CT specimen (fig. 4c, bottom left) indicates the particular case where the ellipse major axis ϕ_r followed the crack propagation direction.

3.3. Finite Element analysis

A porous-visco-plastic constitutive model already implemented in the FE code Zset was used under finite strain formulation (Selles et al. (2017)). The material parameters were optimized thanks to the macroscopic data (δ_c) in fig. 2 as well as the local distribution of V_f. The obtained set of parameters allowed a good agreement between the simulations (lines) and the experimental data (symbols) in fig. 2. Moreover, the porosity contour maps in fig. 4 (top row) were in accordance with those of the measured V_f in fig. 3 (bottom row).

Following then Laiarinandrasana et al. (2016), the principal stresses ($\sigma_{rr}, \sigma_{\theta\theta}, \sigma_{zz}$) were computed and compared with the void characteristic lengths, according to their specific directions. As shown in fig. 4 diagrams, a fair agreement was obtained between the void characteristic lengths and the corresponding FE stress components. It is to be noted that these stress space distributions were obtained at the onset of the tertiary stage, that is at the end of the secondary creep stage. The discussion on the time singularities of the stress is out of the scope of this work.

4. Conclusion

This work considers a semi-crystalline polymer (Polyamide 6) subjected to creep loading with various multiaxial stress states. The effects of the stress triaxiality ratio were investigated using notched round bars NT4 and NT045 (notch root radii of 4 mm and 0.45mm respectively) and a small CT specimen. Additionally to the macroscopic creep opening displacement, the spatial distributions of the void volume fraction, the average void height and diameter (measured by 3D imaging) at the onset of the tertiary creep stage were plotted. It was observed that voids were cylindrical with an elliptical basis. The space evolutions of the void height, major and minor diameters were obtained.

The interpretation of these data in 3D at the microscopic scale was performed in the light of FE analysis in terms of principal stresses. A good agreement was obtained between the void characteristic lengths and the corresponding principal stresses.

References

Laiarinandrasana, L., Morgeneyer, T.F., Proudhon, H., N'Guyen, F., Maire, E., 2012. Effect of Multiaxial Stress State on Morphology and Spatial Distribution of Voids in Deformed Semicrystalline Polymer Assessed by X-ray Tomography. Macromolecules 45, 4658–4668.

Selles, N., N'Guyen, F., Morgeneyer, T.F., Proudhon, H., Ludwig, W., Laiarinandrasana, L., 2016. Comparison of voiding mechanisms in semi-crystalline polyamide 6 during tensile and creep tests. Polymer Testing 49, 137–146.

Selles, N., King, A., Proudhon, H., Saintier, N., Laiarinandrasana, L., 2017. Time dependent voiding mechanisms in polyamide 6 submitted to high stress triaxiality: experimental characterisation and finite element modelling. Mechanics of Time Dependent Materials, 1–21.

Besson, J., Foerch, R., 1997. Large Scale Object-Oriented Finite Element Code Design. Computer Methods in Applied Mechanics and Engineering. 142, 165–187.

Laiarinandrasana, L., Klinkova, 0., N'Guyen, F., Proudhon, H., Morgeneyer, T.F., Wolfgang, L., 2016. Three dimensional quantification of anisotropic void evolution in deformed semi-crystalline polyamide 6. International Journal of Plasticity 83, 19–36.